Modified embedded-atom method interatomic potential and interfacial thermal conductance of Si-Cu systems: A molecular dynamics study

Carolina Abs da Cruz,[1,a)] Patrice Chantrenne,[2,b)] Roberto Gomes de Aguiar Veiga,[2] Michel Perez,[2] and Xavier Kleber[2]
[1]*Université de Lyon, INSA de Lyon, Centre de Thermique de Lyon CETHIL UMR CNRS 5008, Villeurbanne F-69621, France*
[2]*Université de Lyon, INSA de Lyon, MATEIS UMR CNRS 5510, Villeurbanne F-69621, France*

(Received 18 April 2012; accepted 11 December 2012; published online 11 January 2013)

Thermal contact conductance of metal-dielectric systems is a key parameter that has to be taken into account for the design and reliability of nanostructured microelectronic systems. This paper aims to predict this value for Si-Cu interfaces using molecular dynamics simulations. To achieve this goal, a modified embedded atom method interatomic potential for Si-Cu system has been set based upon previous MEAM potentials for pure Cu and pure Si. The Si-Cu cross potential is determined by fitting key properties of the alloy to results obtained by *ab initio* calculations. It has been further evaluated by comparing the structure and energies of Cu dimmers in bulk Si and Cu_mSi_n clusters to *ab initio* calculations. The comparison between MD and *ab initio* calculation also concerns the energy barrier of Cu migration along the (110) channel in bulk Si. Using this interatomic potential, non equilibrium molecular dynamics has been performed to calculate the thermal contact conductance of a Si-Cu interface at different temperature level. The results obtained are in line with previous experimental results for different kind of interfaces. This confirms that the temperature variation of the thermal conductance might not find its origin in the electron-phonon interactions at the interface nor in the quantification of the energy of the vibration modes. The diffuse mismatch model is also used in order to discuss these results. © *2013 American Institute of Physics*. [http://dx.doi.org/10.1063/1.4773455]

I. INTRODUCTION

Copper films deposited on silicon oriented substrates constitute one of the principal combinations in large scale integrated circuits. The number of transistors that can be inserted on an integrated circuit double approximately every two years. As systems become smaller, the interfacial thermal effects between materials becomes preponderant compared to their intrinsic thermal resistance. Miniaturization then creates hot spots that can lead to system failure. Thermal exchanges are also a key point in superlattices developed for thermoelectric conversion. The superposition of dielectric and metal nanolayers can increase the thermoelectric figure of merit because their small size restricts the thermal energy carrier mean free path, thus decreasing the thermal conductivity.[1–3] As a consequence, the understanding of interfacial thermal conductance is critical to develop these systems.

Molecular dynamics (MD) is a useful tool to study atomistic phenomena such as thermal transport through interfaces. However, MD does not take into account electrons, predominant in the analysis of heat transfer in metals. Unless Si is very heavily doped, the tunneling possibility that electrons cross the depletion region of contact is small.[4,5] Then, the role of electron-electron interactions in the thermal transport through the Si-Cu interface is negligible. Moreover, previous theoretical[5,6] and experimental results[7] suggest that the interfacial thermal conductance depends predominantly on the Si/metal lattice interactions, so that heat transfer across the Si-Cu interface can be simulated without considering the contribution of phonon-electrons interactions.

To predict physically meaningful results from atomistic simulations, it is primordial to use reliable interatomic potentials. A reliable interatomic potential should reproduce relevant physical properties of specific elements or alloys, including basic properties such as elastic, structural and defect properties, etc. The methodology developed here is based on previous interatomic potentials[8,9] and the use of MD and molecular statics (MS) simulations whose results are compared to *ab initio* calculations either to fit unknown parameters or to check the versatility of the potential.[10,11]

In the first part of this paper, the interatomic potential choice for bulk material (Si and Cu) is discussed, taking into account harmonic and anharmonic properties for heat transfer simulations. Later on, we will present a new Si-Cu potential based on the fitting of a few properties of selected Si-Cu systems. The Si-Cu potential thus generated is evaluated using MS simulations in order to reproduce the results of *ab initio* calculations for three Cu dimers in bulk Si and seven CuSi clusters. The last test consists in determining the energy barrier for a Cu atom migrating along the (110) channel in bulk Si. Non-equilibrium molecular dynamics (NEMD)[12] simulations with the Si-Cu potential have been carried out to predict the interfacial thermal conductance of Si-Cu systems at different temperatures. These results are compared to the diffuse mismatch model (DMM) in an

[a)]Present address: LITEN/LCH, CEA-Grenoble, 17 rue des Martyrs, 38000 Grenoble, France.
[b)]Electronic mail: patrice.chantrenne@insa-lyon.fr.

attempt to understand the temperature variations of the thermal conductance.

II. INTERATOMIC POTENTIALS FOR Si AND Cu

Heat transfer depends on phonon propagation and interactions in dielectric materials. Thus, the choice of the best potential to predict the thermal conductivity should be based on its ability to recover the material dispersion curves. In a crystalline lattice, phonon interactions are also due to the anharmonic nature of the interactions. The validity of the interatomic potentials can be checked through the variation of the linear expansion with the temperature because thermal expansion is an anharmonic effect.

For Si, Cruz *et al.*[13,14] showed that the 2NN Modified Embedded Atom Method (MEAM) potential gives a better description for both harmonic and anharmonic properties compared to other potentials. In addition, the 2NN MEAM potential gives the results closest to experimental results compared to other formalisms for natural Si thermal conductivity for temperatures ranging from 500 to 950 K.

A reliable description of lattice vibration in copper is also required since experimental and theoretical results[4,6,7] showed a major contribution of phonon(in Si)-phonon(in metal) interactions at the interface compared to phonon(in Si)-electron(in metal) interactions. Thus, the criteria to choose the Cu-Cu interaction potential are the same as those used for Si. Two potentials for Cu-Cu interactions are evaluated: the 1NN MEAM[15] and the 2NN MEAM[16] potential which are also available in the large-scale atomic/molecular massively parallel simulators (LAMMPSs)[17] database. Cu dispersion curves from MEAM interatomic potentials are not available in literature and linear expansion was previously obtained only for temperatures ranging from 273 to 373 K.[16] Thus molecular dynamics simulations are used to determine these characteristic which are important for phonon heat transfer.

A. Dispersion curves from MEAM Cu interatomic potentials

The dispersion relations of Cu were calculated using the velocity-velocity autocorrelation function as described by Papanicolaou.[18] The size of the system was 10 lattice parameters in the three directions. Periodic boundary conditions were used in all directions. Initially, the system was equilibrated for 200 000 time steps in an NVT ensemble, where T is set to the ambient temperature. Afterwards, the simulations were run for more than 200 000 time steps in an NVE calculation with a time step equal to 3 fs. The dispersion curves in the $[\xi, 0, 0]$, $[\xi, \xi, 0]$, and $[\xi, \xi, \xi]$ directions are compared with the experimental dispersion curves for Cu[19] using the 1NN MEAM and 2NN MEAM potentials (Fig. 1).

The 1NN MEAM potential overestimates slightly the transverse modes for large wave vectors. Globally, the 2NN MEAM potentials allow a reproduction of the experimental dispersion curve that is more accurate than the 1NN MEAM potential.[19]

B. Thermal expansion from MEAM Cu interatomic potentials

For the linear thermal expansion, an fcc structure consisting of 108 atoms of copper has been used with periodic boundary conditions in all directions. At 0 K, the volume of the box is determined from MS in order to minimize the potential energy of the system. Then, the system is relaxed in a (NPT) ensemble for 20 ps at different temperatures and time step of 5 fs. At each temperature, the average volume of the simulation box is divided by the volume at 0 K. This ratio is calculated with the 1NN MEANM and 2NN MEAM potentials for Cu-Cu interactions and is compared to the experimental ratio[20] in Fig. 2.

When the temperature increases, the 2NN MEAM potential predicts the expansion coefficient for Cu quite accurately while 1NN MEAM potential significantly

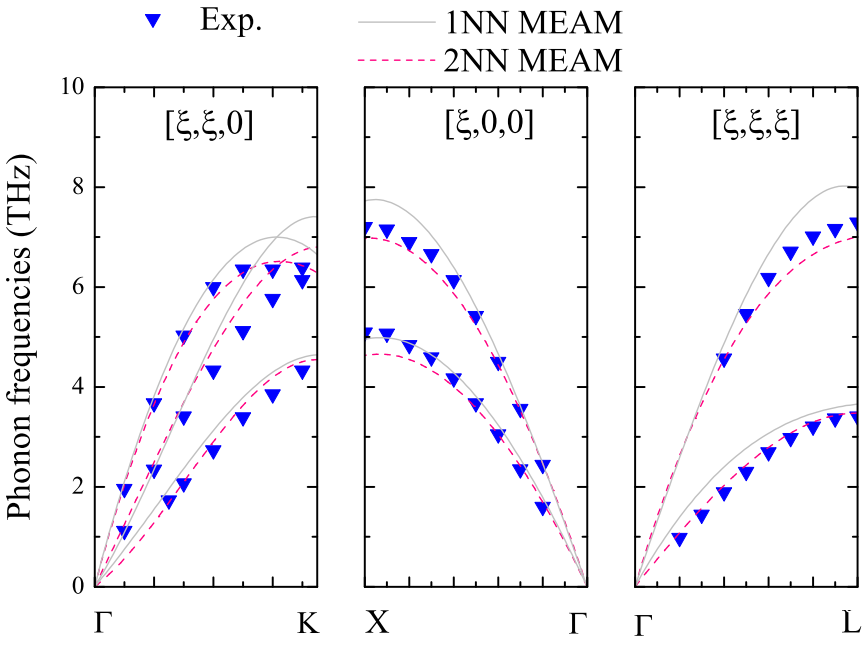

FIG. 1. Phonon dispersion curves using the 1NN MEAM and 2NN MEAM potentials for Cu compared to experimental results[19].

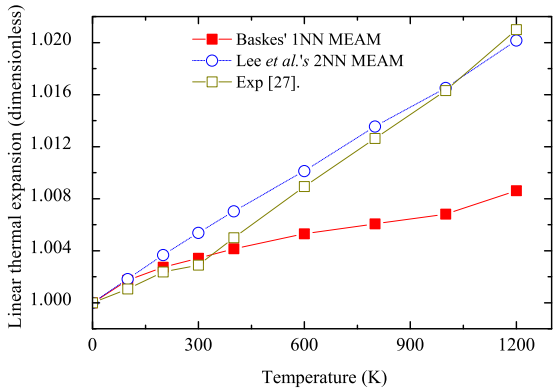

FIG. 2. Relative volume variation of Cu function of the temperature level using the 1NN MEAM and 2NN MEAM potentials and compared to experimental results.[21]

underestimates it. Even if the 1NN MEAM potential gives results closer to the experimental values for the linear thermal expansion at room temperature, the values obtained for the linear thermal expansion for temperatures higher than the room temperature are not reasonable.

Therefore, considering the dispersion curves and the thermal expansion criteria, the 2NN MEAM potential is better to simulate phonon heat transfer in Cu compared to the 1NN MEAM potential.

As a result, we developed a cross-potential based on the 2NN MEAM potential for Si[22] and Cu.[16]

III. DETERMINATION OF THE CROSS POTENTIAL PARAMETERS FOR THE Si-Cu INTERACTIONS

The choice of the same kind of interatomic potentials for Si and Cu is quite convenient. These potentials have been extensively described previously even for alloys.[15,16,22,23]

For an alloy, nine parameters have to be determined for the cross potential parameters:

- four of them appear in the equation of state, namely, E_i^0, cohesive energy, a_0 is the equilibrium lattice parameter, B, the bulk modulus, and d, an adjustable parameter.
- four screening coefficients $C_{min}(i,k,j)$ which define the extent of screening for an atom k to interactions between atoms i and j. For Si-Cu alloy, $C_{min}(i,k,j)$ stand for C_{min}(Si, Cu, Si), C_{min}(Cu, Si, Cu), C_{min}(Si, Si, Cu), and C_{min}(Si, Cu, Cu). Using the 1NN MEAM formalism, all the $C_{min}(i,k,j)$ are taken equal to 2.0.[15] In the 2NN MEAM formalism, the second nearest-neighbor interactions are included adjusting the values of $C_{min}(i,k,j)$ parameters, usually lower than 2.0.
- the density scaling factor ratio, $\frac{\rho_{Si}^0}{\rho_{Cu}^0}$. The electron density scaling factor does not change the energy of pure crystals, but affect interactions between Cu and Si atoms.[8,11]

The determination of E_i^0, a_0, and B is based on the comparison of MS and density functional theory (DFT) within the local density approximation (LDA) calculations on a L12 Cu_3Si alloy. The geometry optimisation with MS is obtained using the conjugate gradient (CG) algorithm[24] within the LAMMPS code.[17] *Ab initio* calculations in the framework of the LDA were performed with the SIESTA code,[25] which uses a localized linear combination of atomic orbitals (LCAO) as basis set in order to solve the Kohm-Sham equations. A double-ζ basis set with polarization functions (DZP) optimized for both bulk Cu[26] and Si[25,26] with the corresponding norm-conserving pseudopotentials is considered in the calculations. A cutoff of 4080 eV for the grid integration was employed to represent the charge density. The geometry optimization with SIESTA was also performed by the CG algorithm. This leads to $E_i^0 = 4.5$ eV, $a_0 = 3.6$ Å, and $B = 152$ GPa.

C_{min}(Cu, Si, Cu) and C_{min}(Si, Cu, Si) are taken equal to the values proposed by Lee's[16] and Lee *et al.*'s[22] potentials for pure Cu and Si. C_{min}(Cu, Cu, Si), C_{min}(Cu, Si, Si), and d have been obtained based on the same assumptions of Lee *et al.* for the screening function parameter values using an L12 structure for the Fe-Cu binary system.[8] These parameters are listed in Table I.

The density scaling factor ratio parameter, $\frac{\rho_{Si}^0}{\rho_{Cu}^0}$, is related to the enthalpy variation of the crystal of one species when an atom of the other species is inserted as an impurity, usually substitutional. Nevertheless, Baker *et al.*[27] observed experimentally that Cu impurities can be found occupying both substitutional and interstitial sites in bulk Si. Therefore, $\frac{\rho_{Si}^0}{\rho_{Cu}^0}$ is fitted in order to minimize the difference between the substitution and interstitial impurity energies given by MS and DFT calculation. The best fit leads to $\frac{\rho_{Si}^0}{\rho_{Cu}^0} = 1.8$. With this value, Table II compares the formation energies obtained by *ab initio* calculations and the MEAM potential for a Si atom substitutional in Cu fcc (E_1) and for a Cu atom substitutional (E_2) and interstitial (E_3) in Si diamond.

Ryu and Cai[11] had previously discussed the difficulty in choosing a scaling factor ratio parameter for a Si-Au system such that all configuration energies paired with the DFT results. We faced the same problem with the MEAM Si-Cu potential presented in this study: if $\frac{\rho_{Si}^0}{\rho_{Cu}^0}$ increases, then E_1 increases and E_2 and E_3 decrease, and vice-versa.

IV. TESTING THE VERSATILITY OF THE Si-Cu INTERATOMIC POTENTIAL

An important issue in potential derivation concerns the fact that the validation procedures usually focus on condensed phase systems consisting of defect free or low defect concentration environments. This casts doubt on the potential transferability, i.e., its ability to yield good results when the atomic coordination in the system under study strongly differs from what is found in a perfect or quasi-perfect crystal. As interface is of interest in this study, several configurations are considered in this section.

TABLE I. C_{min} and d parameters for the Si-Cu cross potential.

Parameters	Values
C_{min}(Cu,Si,Cu)	1.21
C_{min}(Si,Cu,Si)	1.41
C_{min}(Cu,Cu,Si)	1.30809
C_{min}(Cu,Si,Si)	1.30809
d	0.0375

TABLE II. The formation energies of Si (Cu) impurities in Cu fcc (Si diamond) obtained by the MS potential and DFT-LDA calculations.

	DFT-LDA	MS
E_1 (eV)	0.64	0.66
E_2 (eV)	2.35	1.14
E_3 (eV)	1.47	1.86

TABLE III. DFT-LDA and MS-obtained formation energies of the CuSi small clusters.

	DFT-LDA	MS	Difference (%)
CuSi	3.49	3.94	11
$CuSi_2$	2.33	2.50	7
Cu_2Si	2.77	2.16	28
$CuSi_3$	2.53	2.36	7
Cu_3Si	1.92	2.26	15
Cu_2Si_2 (a)	1.92	2.03	5
Cu_2Si_2 (b)	2.25	2.16	4

A. Single impurities

First, we have calculated some geometrical properties of Cu (respectively Si) as an impurity in bulk Si (respectively, Cu), namely, the Si-Cu bond lengths and the angles between the impurity and its first nearest neighbors (see Table IV). As one can see, the only remarkable difference concerns the bond length when the Cu atom replaces a Si atom in the diamond crystal: the MS result is about 10% smaller than the value given by LDA. For all other results, the difference between LDA and MS is less than 1%.

B. Small Si-Cu clusters

Clusters represent an extreme case, since we may have covalent bonds between atoms of metallic elements and also dangling bonds, two features that might be observed in high defective environments. Owing to their small size, such 0D atomic arrangements are also convenient systems for potential validation because their properties can be calculated very quickly by *ab initio* methods.

The formation energies per atom and relaxed geometries of seven isolated CuSi clusters (see Fig. 3) were obtained using the MS and *ab initio* calculations. The results are summarized in Tables III and IV. For the formation energies, the differences between the *ab initio* and MS results are lower than 15% for all clusters except CuSi. Moreover, except for the geometry of CuSi, MS reproduces the geometries obtained by *ab initio* calculations reasonably well.

C. Cu dimers in bulk Si

Experimental results showed that Cu dimer-vacancy complexes were formed after Cu deposition on Si surfaces and subsequent incorporation into the submonolayers.[27,28] Motivated by the experimental findings, three Cu dimers were introduced in the Si structure in order to test the ability of the MEAM potential to model a more complex impurity configuration than in Secs. V A and V B (i.e., taking into account impurity-impurity interactions):

1. an interstitial and a substitutional Cu atom (D1);
2. two interstitial Cu atoms (D2);
3. two substitutional Cu atoms (D3).

The formation energies as well as the Cu-Cu distances of the three dimer configurations can be seen in Fig. 4. Additionally, some dimer geometrical properties as first nearest neighbours distances and angles are shown in Table V. The only noticeable discrepancy between DFT and MEAM regards the formation energy of D3 (about 60%). In general, the MEAM-DFT agreement is within 10%.

D. Energy barrier for Cu migration in bulk Si

Cu contamination through the surface-to-bulk diffusion is an important issue in Si-Cu contacts.[27–30] Hence, we tested the ability of the MEAM potential to predict the energy barrier for Cu migration in bulk Si. The energy barrier for a neutral Cu atom migrating in the (110) channel in bulk Si was calculated from molecular statics simulations and *ab initio* calculations. The Cu atom is expected to occupy a tetrahedral site in Si diamond (local energy minimum). When it jumps to an adjacent tetrahedral site, it passes through a hexagonal site (saddle point) in the middle of the minimum energy path. The geometries of these two interstitial sites are depicted in Fig. 5. The energy barrier is the difference in the total energies of the system corresponding to the Cu atom sitting on these two interstitial sites. The MEAM potential

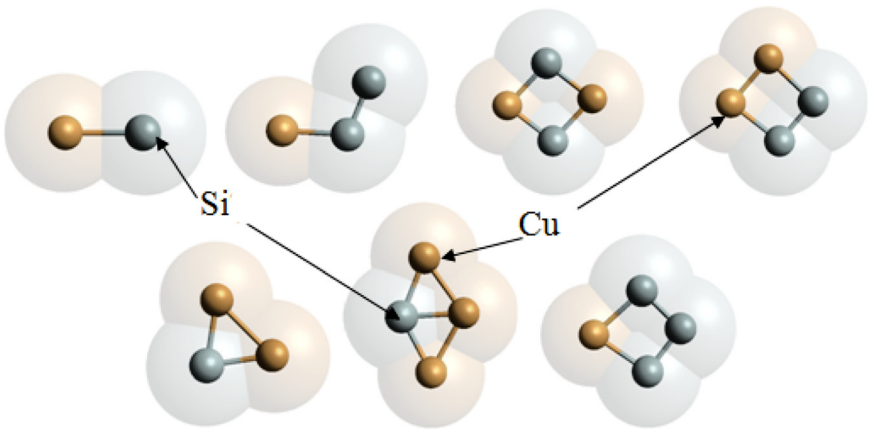

FIG. 3. CuSi clusters considered in this study.

TABLE IV. DFT-LDA and MS-obtained bond lengths and angles of the CuSi small clusters.

	R (Å)		θ (°)	
	DFT-LDA	MS	DFT-LDA	MS
CuSi	2.2	2.7		
$CuSi_2$	2.2	2.4 and 3.7	58	32
Cu_2Si	2.2	2.4	68	73
$CuSi_3$	2.2 and 3.0	2.6 and 3.4	48	38
Cu_3Si	2.2	2.3	60	66
Cu_2Si_2 (a)	2.3	2.1	60	64
Cu_2Si_2 (b)	2.3	2.0	60	64

provided a value of 0.31 eV for the migration energy of a Cu atom in Si diamond, paired extremely well with the *ab initio* value (0.33 eV) and paired well with the experimentally obtained value of Heiser and Mesli (0.39 eV).[30]

V. INTERFACIAL THERMAL CONDUCTANCE OF Si-Cu SYSTEMS

The interfacial thermal conductance G_K has been predicted with NEMD simulations employing the newly developed Si-Cu MEAM potential for average temperatures ranging from 200 K to 500 K and using DMM for two average temperatures: 300 and 400 K.

A. MD methodology

To perform NEMD, the temperature gradient is obtained by means of a hot and a cold thermostated zone at the top and the bottom of the system in the z direction, respectively. The velocity rescale method[31,32] is used to maintain a fixed temperature at the cold and hot zones. The thickness of the thermostated zones is equal to 1 lattice parameter. When the steady state is reached, the kinetic energy difference before and after rescaling at each time step in the hot and the cold zones $\Delta E_h(i)$ and $\Delta E_h(i)$, respectively, is used to calculate the heat flux, Q,

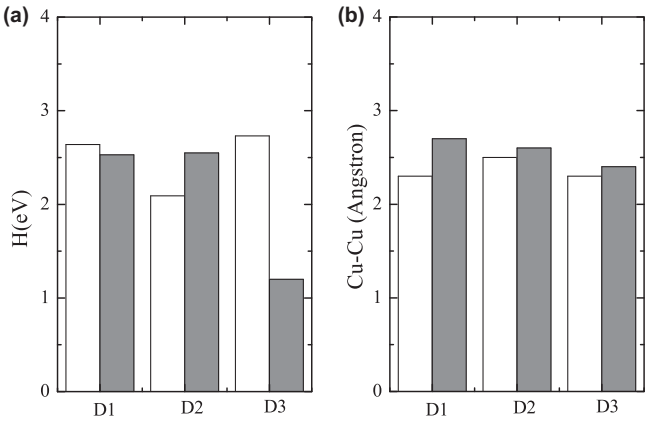

FIG. 4. Dimer formation energies per atom (a) and Cu-Cu distances (b) obtained with the MS (gray bars) and DFT-LDA calculations (white bars).

TABLE V. DFT-LDA and MS-obtained Si-Cu bond lengths and angles for the Cu dimers in bulk Si (where we have Cu substitutional (Cu_S) and interstitial (Cu_I)).

	R_{SiCu} (Å)		θ (deg)	
	DFT-LDA	MS	DFT-LDA	MS
$Cu_{S,D1}$	2.5	2.3	106	104
$Cu_{I,D1}$	2.2	2.3	111	110
$Cu_{I,D2}$	2.5	2.3	103 and 116	116
$Cu_{S,D3}$	2.3	2.4	110	109

$$Q = \sum_{i=1}^{n} \frac{\Delta E_h(i) + \Delta E_c(i)}{A \times 2 \times \Delta t \times n}, \tag{1}$$

where A is the area of the section crossed by heat between the hot and cold thermostated zones.

Initially, the system was equilibrated with a constant pressure of 1 atm for 25 ps with a time step of 0.5 fs. Afterwards, a Si and Cu layer, one lattice parameter thick, had been maintained fixed below and above the thermostated zone, respectively, to avoid a system instability in a fixed volume NEMD simulation. Then, the simulation is run for more than $n = 2 \times 10^6$ time steps for the statistic to predict interfacial thermal conductance G_K. The interface thermal conductance, creates a discontinuous temperature, ΔT, and a barrier to heat flux across the interfaces. It is defined by

$$Q = \Delta T \times G_k. \tag{2}$$

Our model structure consisted of a slab of diamond Si (7488 atoms) in contact with a slab of fcc Cu (7128 atoms). The two slabs are in contact within a rectangular box of cross-section $A = 32.58 \times 32.58$ Å^2 and a length of 222 Å. The distance between Si and Cu crystals is set at 0 K to reach a local energy minimum. Periodic boundary conditions are used x and y directions and free boundary condition are used in the heat transfer direction (z).

The simulation box was divided into slices of 1 lattice parameter thick and near to the interface, 6 slices were 2 atomic layers thick (equal to 1.35 Å for Si and 1.8 Å for Cu). When the temperature profile is linear for both materials, a linear fit can be made for both materials and ΔT is obtained by looking at the difference between the two linear fits at the interface.[33] When the intermixing zone is considerable,

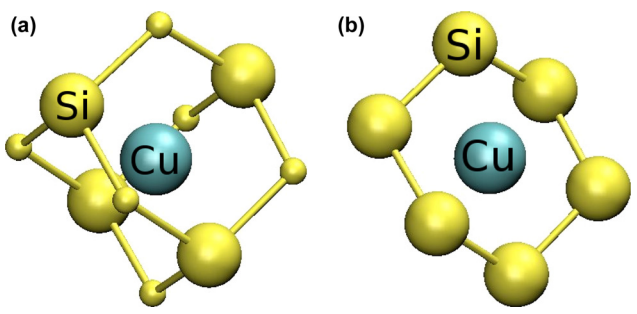

FIG. 5. Tetrahedral (a) and hexagonal (b) sites occupied by a Cu atom in bulk Si.

phonon interfacial conductance is usually decomposed into boundary and interfacial-region conductances.[5] In our simulations, the temperature profiles are not linear due to the interface restructuring and ballistic behavior of phonons in Si crystal. Moreover, the interface mixing is not significant enough (at 500 K the intermixing zone of Si and Cu atoms is 2.0 Å) to decompose the system into two different zones. Then, the temperature of the first and the second slice near the interface for Si and Cu (two slices, each with a thickness of 5.43 Å each one before relaxation) was averaged to obtain the temperature drop. This criterion had been used for all temperatures.

Simulations are run to get a temperature drop in the interface being nearly 10% of the mean temperature value[32] which leads to a difference between the first and second layer temperatures less than 5% that allows acceptable error bars. The uncertainty is calculated using the following expression:

$$\sigma G_K = G_K \times \left(\frac{\sigma Q}{Q} + \frac{\sigma(\Delta T)}{\Delta T} \right), \tag{3}$$

where $\sigma(\Delta T)$ is equal to

$$\sigma(\Delta T) = \sqrt{(\sigma T_{Si})^2 + (\sigma T_{Cu})^2}. \tag{4}$$

The uncertainty of the Q value is negligible compared to the uncertainty of the temperature drop. As the average temperature of two layers has been used to determine G_K, the uncertainty should recover the error bars for temperature gradients of first and second slices at the interface of each material, σT_{Si} and σT_{Cu}. For temperatures around room temperature, the temperature difference between first and second layers are nearly 1%. For high temperatures, this difference is nearly 4% increasing the G_K uncertainty.

Wherever the phonon-mean free path is comparable with the system size, the thermal conductivity values obtained from MD simulations depend on the simulation box size.[12,31] However, it has been shown that the size effects are less significant for G_K.[32,34] This has been checked simulating heat transfer on an extended system (by about 50%) in the heat current direction at 300 K. The total length of the extended structure was 346 Å.

B. Results

Fig. 6 shows the temperature profile for the Si-Cu system for the smaller and larger system size in the heat transfer direction for a mean temperature equal to 300 K.

The values of interfacial thermal conductances at 300 K are equal to (234 ± 25) MW/(m^{2}K) and (263 ± 40) MW/(m^{2}K) for the smaller and larger systems, respectively. For the larger configuration, the relative error is greater than 10%, and it still falls within the uncertainty range of a smaller structure. So, we consider that size effects are no significant. The temperature profile for Si is almost flat due to its high thermal conductivity. With MD simulations it is not possible to simulate heat transfer due to the electrons, thus the high temperature gradient in Cu is due to its low lattice thermal conductivity.

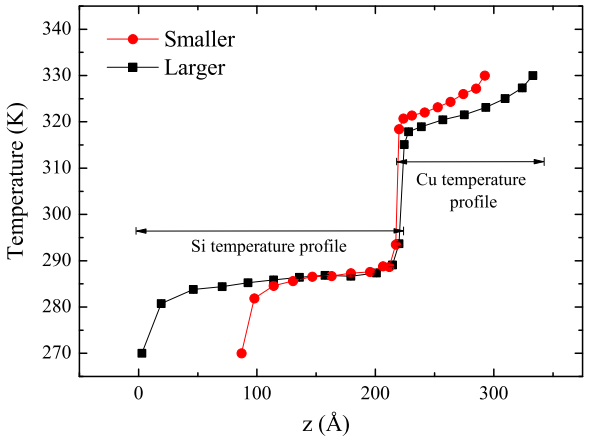

FIG. 6. Temperature profile for the Si-Cu system modelled by NEMD.

The temperature dependence of the Si-Cu interfacial thermal conductance, G_K, is plotted in Fig. 7. Note that the temperature level is the mean value of the hot and cold thermostated zones. G_K is in the range 8–700 MW/(m^{2}K) of the Kapitza conductance for dielectric/metal systems.[35,36] G_K significantly increases (variations much larger than the uncertainties) for temperatures larger than 300 K. Hu *et al.*[32] and Luo and Lloyds[34] already reported temperature increase of the Kapitza conductance (predicted by NEMD) for Si-polymer and for Au/SAM interface respectively. Although the variations were less important, experimental results[37] also exhibit such trends for the Kapitza resistance of a metal-dielectric (Al/Al_2O_3) interface.

Despite MD simulations do not account for electron-phonon interactions, we observe a good agreement between our results and previous experimental[7] and theoretical[4–6] results. This confirms that phonon-phonon interactions are much more significant than electron-phonon and electron-electron interactions at the semiconductor/metal interface.

In the system studied by Hopkins *et al.*,[37] the Al_2O_3 and Al Debye temperatures are 1043 K and 428 K, respectively. The Debye temperature ratio is equal to 2.4. The Kapitza conductance variations might be correlated with quantum effects since the temperature range is much below the Al_2O_3

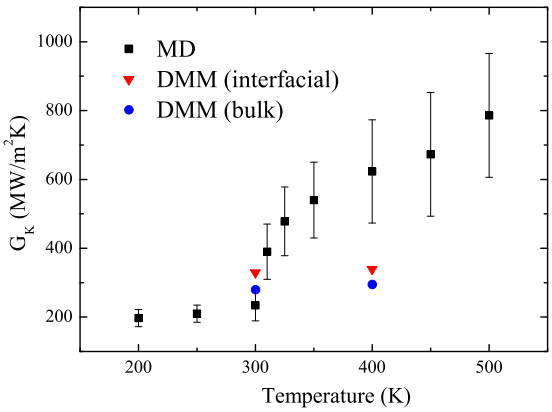

FIG. 7. Interfacial thermal conductance as a function of temperature determined from MD and DMM. DMM fails to predict interfacial thermal conductance for temperatures higher than 300 K, whatever the zone where density of states is considered.

Debye temperature and around the Al Debye temperature. In our case, the silicon and copper Debye temperatures are 645 K and 343 K, respectively. The Debye temperature ratio is equal to 1.9. The interfacial thermal conductance is calculated between 200 and 500 K, which is around the copper Debye temperature and below the Si Debye temperature. However, NEMD do not take into account of the quantification of energy on the vibration modes. Thus one might conclude that the Kapitza conductance temperature variations are not due to quantum effect. This motivates the discussion in Sec. V C which aims to investigate this tendency using the classical diffuse mismatch model.

C. Discussion

In this section, the diffuse mismatch model is used in order to investigate the temperature variations of the Si-Cu Kapitza resistance. Considering the phonon group velocity and the phonon density of state, D, the transmission probability from Si to Cu[5] in the DMM is

$$\tau_{Si\to Cu}(\omega) = \frac{u_{Cu}D_{Cu}(\omega)}{u_{Si}D_{Si}(\omega) + u_{Cu}D_{Cu}(\omega)}, \tag{5}$$

where ω is the phonon frequency. The phonon group velocity u is averaged from transverse and longitudinal group velocities. These group velocities were obtained from the Si[22] and the Cu[16] bulk elastic constants. This formulation for $\tau_{1\to 2}(\omega)$ allows only elastic scattering. Then, if a specific phonon frequency does not exist in Si, even if it exists in Cu, or vice versa, it cannot participate in interfacial transport.

In our case, the average group velocity of the transverse and the longitudinal branches were used to calculate the interfacial thermal conductance, G_K, given by[5]

$$G_K = \frac{Q}{T_{Si} - T_{Cu}} = \frac{1}{4}\int_{\omega=0}^{\omega_m} \frac{[f(\omega, T_{Si}) - f(\omega, T_{Cu})]}{T_{Si} - T_{Cu}} \times D_{Si}(\omega)\hbar\omega u_{Si}\tau_{Si\to Cu}(\omega)d\omega, \tag{6}$$

where ω_m is the cut-off frequency and f is the Bose-Einstein distribution. The used transmission probability is the one obtained with the DMM from Eq. (5).

Equations (5) and (6) assume that there is a local thermal equilibrium at the interface and take into account the energy quantification on the vibration modes. They have to be modified in order to match the NEMD simulation conditions. Equation (6) is modified using the high temperature limit of the Bose-Einstein distribution function even if interfacial temperatures T_{Si} and T_{Cu} are below the Debye temperature. This ensures having the classical energy distribution on the vibration modes. Thus, the temperature dependence of G_K only appears through the density of state and transmission coefficient,

$$G_K = \frac{1}{4}\int_0^{\omega_m} k_b D_{Si}(\omega)u_{Si}\tau_{Si\to Cu}(\omega)d\omega. \tag{7}$$

The transmission coefficient might be calculated considering a different temperature level on each side of the interface and thus a different vibration mode population given by the Bose Einstein distribution function. The expression below is derived from a detailed balance at the interface as proposed by Swartz,[38]

$$\tau_{Si\to Cu}(\omega) = \frac{f(\omega, T_{Cu})u_{Cu}D_{Cu}(\omega)}{f(\omega, T_{Si})u_{Si}D_{Si}(\omega) + f(\omega, T_{Cu})u_{Cu}D_{Cu}(\omega)}. \tag{8}$$

Using the high temperature limit of the Bose Einstein Distribution function leads to

$$\tau_{Si\to Cu}(\omega) = \frac{T_{Cu}u_{Cu}D_{Cu}(\omega)}{T_{Si}u_{Si}D_{Si}(\omega) + T_{Cu}u_{Cu}D_{Cu}(\omega)}. \tag{9}$$

Considering Eqs. (9) and (6), the temperature variations of the Kapitza conductance might be due to the temperature difference between the interface temperature in Cu and Si, but also to the density of state temperature variations. It has already been shown that the bulk and interfacial density of states are different. Thus, these two density of states are determined to calculate the kapitza conductance.

D is calculated via a Fourier transform of the atomic velocity autocorrelation function.[39] Three lattice parameters in the central region along the z direction of each material are considered for the determination of D. When the steady state is reached the simulations were run for more than $n = 300\,000$ time steps with an integration time step of 0.01 fs and the velocity acquisition of the atoms in the central zone of the Si and the Cu layers was performed every 20 time steps. The vibrational spectra for bulk Si and Cu at 300 K and at 400 K do not exhibit significant differences.

As the temperature variations of the bulk density of state D is not significant, D_{Cu} and D_{Si} are then determined in the interfacial zone using the Fourier transform of the velocity autocorrelation function of two atomic layers in Si just below the theoretical interface and two atomic layers in Cu just above the interface. Interfacial density of state is distorted compared to bulk density of state (Fig. 8) due to the interpenetration of the force fields.[5] The atomic restructuring and bond interactions provide additional phonon modes for Si. D shows a pic reduction for optical phonon modes and higher

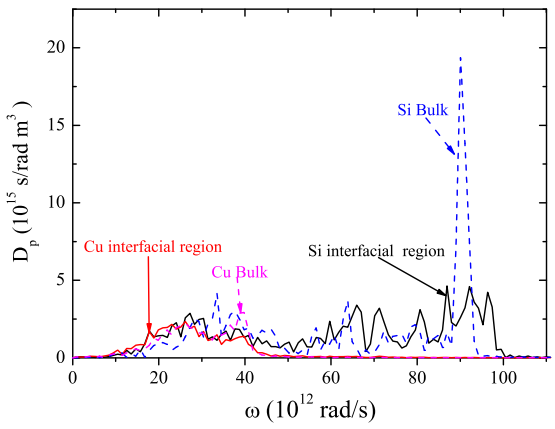

FIG. 8. The vibrational density of state spectra for the Si-Cu system in the bulk material and interfacial region at 300 K determined from NEMD via a Fourier transform of the atomic velocity.

frequency phonon modes participate at the boundary compared to the bulk. D_{Cu} shifts to lower energies while D_{Si} shifts to higher energies.

Using Eqs. (5) (local equilibrium at the interface) and (7) and the bulk density of state, which does not change between 300 and 400 K, G_K is equal to 316 MW/(m^{2}K) at 300 K and at 400 K. As expected in these conditions, G_K does not depend on the temperature level. Using the interfacial density of state which exhibits slight temperature variation, G_K now equals 343 MW/(m^{2}K) at 300 K and 351 MW/(m^{2}K) at 400 K. The use of these interfacial densities of state in the DMM simply increases interfacial thermal conductance by adding phonon modes and shifting frequencies as predicted by Shin *et al.*[5]

To take into account of the temperature difference at the interface between Cu and Si, Eqs. (7) and (9) are used to calculate G_K. Using the bulk density of state: $G_K = 336$ MW/(m^{2}K) at 300 K and $G_K = 332$ MW/(m^{2}K) at 400 K. Using the interfacial density of state, $G_K = 365$ MW/(m^{2}K) at 300 K and $G_K = 370$ MW/(m^{2}K) at 400 K.

Temperature induced variations of the thermal conductance are still negligible. Thus, the temperature variations of either the bulk or the interfacial D_p cannot explain the temperature variations of G_K.

The difference between the DMM and MD results might be due to the fact that the transmission coefficient at the interface is determined using bulk phonon group velocities despite the fact that we had been using interfacial D. As the force field distorts the density of states, phonon group velocities might also be affected, changing the transmission coefficient and the interfacial thermal conductance. However, as the density of state does not vary significantly when the temperature increases, this is also certainly the case for the group velocity.

These results tend to confirm the importance of the inelastic contribution to the interfacial conductance as already mentioned by several authors.[33,37,40,41] Duda *et al.*[42] used complete bulk dispersion curves to calculate the elastic and inelastic scattering contribution of phonons to the interfacial thermal conductance using the DMM. They showed that the transmission coefficient increases with the temperature when inelastic scattering is considered and all phonons on both sides of the interface can participate in interfacial transport processes. An increasing of the transmission coefficient value leads to an increase of G_K.

At the moment, MD is the only theoretical tool that shows the experimental sharp trends for G_K with the temperature because it accounts for naturally phonon modes and multiple-phonon processes (both elastic and inelastic scattering) at the interface.

VI. CONCLUSIONS

Heat transfer across interfaces, characterized by a thermal contact conductance, is a crucial issue when dealing with nanostructured materials. Measurement of such quantity is still a challenge and experimental results are quite limited, which motivates efforts towards accurate theoretical prediction. Previous experimental and theoretical studies demonstrated that the phonon (in dielectric material)-phonon (in metal) interactions are the main contributor to heat transfer across a dielectric-metal interface. Thus in this paper, molecular dynamics was used to predict the thermal conductance of a Si/metal interface in the particular case for which the metal is copper.

The two main properties that need to be accurately reproduced with an interatomic potential for heat transfer simulations are the dispersion curve and the dilatation coefficient. Second nearest neighbour MEAN potentials for Si and for Cu were validated on these two criteria.

A cross potential for Si-Cu interactions has been put forward. It has been tested on the heat of formation and the relaxed geometries of seven Cu_mSi_n clusters, and then successfully compared to *ab initio* calculations. Moreover, three Cu dimers were introduced into bulk Si and the corresponding heat of formation and relaxed geometries were also successfully compared to *ab initio* calculations. As Cu diffusion into the Si bulk is also an important issue, the migration energy for Cu in bulk Si (between the tetrahedral site and the saddle point) has been calculated. A value of 0.31 eV has been found, pairing extremely well with the *ab initio* prediction (0.33 eV).

The predicted interfacial thermal conductance is (263 ± 40) MW/(m^{2}K) at 300 K, which is in the range 8–700 MW/m^{2}K encountered in the literature[35,36] for dielectric/metal systems. For temperatures around the metal Debye temperature, the interfacial thermal conductance increases sharply, a feature that was already observed in experimental works on dielectric/metal systems.[37] The results are also consistent with previous theoretical results for dielectric/metal interfacial thermal conductance,[4,6,7] which demonstrated that phonon-phonon interactions contribute much more to heat transfer than electron-phonon interactions.

It was demonstrated that the diffuse mismatch model failed to describe the temperature dependence of the interfacial thermal conductance (even when interfacial density of state is used). Two hypotheses could explain this discrepancy: (i) DMM considers the bulk phonon group velocity, which might be modified by the interface. As the density of state does not change function of the temperature, this might not have a strong influence on the thermal conductance (ii) inelastic effects that would allow mode conversion between modes that are not taken into account with the DMM. This assumption is the one that has been expressed many times in the literature and that might be the most probable. Up to now, only molecular dynamics is able to exhibit this temperature trend of the interfacial thermal conductance. In the case of Si-Cu system, this temperature variation is particularly important compared to what has been observed on other systems (Si/Ge, Si/polymer). This phenomenon is worth to be experimentally studied to confirm the prediction. This is quite interesting because its understanding could be an opportunity for thermal diode applications.

ACKNOWLEDGMENTS

This work was funded by the CNRS in the framework of the ANR-New researchers NanoMetrEther and the ANR COFISIS projects, ANR-07-NANO-047-03. The authors are

grateful for the use of the extensive computer facilities; CNRS-IDRIS and the P2CHPD of the FLCHP (Fédération Lyonnaise de Calcul Haute Performance).

[1]D. Vashaee and A. Shakouri, J. Appl. Phys. **95**, 1233 (2004).
[2]D. Vashaee and A. Shakouri, Phys. Rev. Lett. **92**, 106103 (2004).
[3]K. Termentzidis, J. Parasuraman, C. A. Cruz, S. Merabia, D. Angelescu, F. Marty, T. Bourouina, X. Kleber, P. Chantrenne, and P. Basset, Nanoscale Res. Lett. **6**, 288 (2011).
[4]A. Kikuchi, Phys. Status Solidi A **175**, 623 (1999).
[5]S. Shin and M. Kaviany, Phys. Rev. B **82**, 081302 (2010).
[6]J. D. Mahan, Phys. Rev. B **79**, 075408 (2009).
[7]H.-K. Lyeo and D. G. Cahill, Phys. Rev. B **73**, 144301 (2006).
[8]B.-J. Lee, B. D. Wirth, J.-H. Shim, J. Kwon, S. C. Kwon, and J.-H. Hong, Phys. Rev. B **71**, 184205 (2005).
[9]B.-J. Lee, Acta Mater. **54**, 701 (2006).
[10]C.-L. Kuo and P. Clancy, Surf. Sci. **551**, 39 (2004).
[11]S. Ryu and W. Cai, J. Phys.: Condens. Matter. **22**, 055401 (2010).
[12]P. K. Schelling, S. R. Phillpot, and P. Keblinski, Phys. Rev. B **65**, 144306 (2002).
[13]C. A. Cruz, K. Termentzidis, X. Kleber, and P. Chantrenne, J. Appl. Phys. **110**, 034309 (2011).
[14]C. A. Cruz, P. Chantrenne, and X. Kleber, J. Heat Transfer **134**, 062402 (2012).
[15]M. I. Baskes, Phys. Rev. B **46**, 2727 (1992).
[16]B.-J. Lee, J.-H. Shim, and M. I. Baskes, Phys. Rev. B **68**, 144112 (2003).
[17]S. Plimpton, J. Comput. Phys. **117**, 1 (1995).
[18]N. I. Papanicolaou, I. E. Lagaris, and G. A. Evangelakis, Surf. Sci. **337**, L819 (1995).
[19]R. M. Nicklow, G. Gilat, H. G. Smith, L. J. Raubenheimer, and M. K. Wilkinson, Phys. Rev. **164**, 922 (1967).
[20]Y. S. Touloukian, R. E. Taylor, and P. D. Desai, *Thermal Expansion-Metallic Elements and Alloys* (Plenum, New York, 1975), Vol. 12.
[21]Y. S. Touloukian, R. K. Kirbi, R. E. Taylor, and T. Y. R. Lee, *Thermophysical Properties of Matter* (Plenum, New York, 1977), Vol. 13.
[22]B.-J. Lee, Comput. Coupling Phase Diagrams Thermochem. **31**, 95 (2007).
[23]B.-J. Lee and M. I. Baskes, Phys. Rev. B **62**, 8564 (2000).
[24]Y. Saad, *Iterative Methods for Sparse Linear Systems*, 2nd ed. (Philadelphia, 2003).
[25]J. M. Soler, J. D. Gale, J. J. A. García, P. Ordejón, and D. Sanchéz-Portal, J. Phys.: Condens. Matter **14**, 2745 (2002).
[26]J. Junquera *et al*., Phys. Rev. B **64**, 235111 (2001).
[27]L. A. Baker, A. R. Laracuente, and L. J. Whitman, Phys. Rev. B **71**, 153302 (2005).
[28]H. Bracht, Mater. Sci. Semicond. Process. **7**, 113 (2004).
[29]J. Hohage, U. Mayer, M. U. Lehr, F. Feustel, O. Aubel, and C. Hennesthal, Microelectron. Eng. **87**, 2119 (2010).
[30]T. Heiser and A. Mesli, Appl. Phys. A **57**, 325 (1993).
[31]P. Chantrenne, J. L. Barrat, X. Blase, and J. D. Gale, J. Appl. Phys. **97**, 104318 (2005).
[32]M. Hu, P. Keblinski, and P. Schelling, Phys. Rev. B **79**, 104305 (2009).
[33]R. J. Stevens, L. V. Zhigilei, and P. M. Norris, Int. J. Heat Mass Transfer **50**, 3977 (2007).
[34]T. Luo and J. R. Lloyd, Int. J. Heat Mass Transfer **53**, 1 (2010).
[35]H. Smith, J. L. Hostetler, and P. M. Norris, Microscale Thermophys. Eng. **4**, 51 (2000).
[36]R. J. Stoner and H. J. Maris, Phys. Rev. B **48**, 16373 (1993).
[37]P. E. Hopkins, P. Norris, and R. J. Stevens, ASME Trans. J. Heat Transfer **130**, 022401 (2008).
[38]E. Swartz, Rev. Mod. Phys. **61**, 605 (1989).
[39]L. V. Zhigilei, D. Srivastava, and B. J. Garrison, Surf. Sci. **374**, 333 (1997).
[40]Y. Chen, D. Li, J. Yang, Y. Wu, J. R. Lukesd, and A. Majumdare, Physica B **349**, 270 (2004).
[41]E. S. Landry and A. J. H. McGaughey, Phys. Rev. B **80**, 165304 (2009).
[42]J. C. Duda, T. E. Beechem, J. L. Smoyer, P. M. Norris, and P. E. Hopkins, J. Appl. Phys. **108**, 073515 (2010).